17th World Conference on Earthquake Engineering, 17WCEE
Sendai, Japan - September 13th to 18th 2020

HYSTERETIC BEHAVIOR OF SHS STEEL COLUMNS SUBJECTED TO SMALL AMPLITUDE LOADING HISTORY

T. Ishida[(1)], S. Yamada[(2)]

[(1)] *Assistant Professor, Tokyo Institute of Technology, ishida.t.ae@m.titech.ac.jp*
[(2)] *Professor, Tokyo Institute of Technology, yamada.s.ad@m.titech.ac.jp*

Abstract

Structural components may be subjected to a relatively small amplitude and a large number of cyclic loading under long-duration and long-period earthquake excitations as well as multiple strong ground motions in a short period of time such as the 2016 Kumamoto Earthquake. Lower ends of columns of 1st story would yield under severe earthquake, even though the strong-column-weak-beam concept is adopted in the design. Therefore, deformation capacities and hysteretic behaviors including the strength deterioration range of steel columns subjected to small amplitude cyclic loads should be clarified to evaluate seismic performance of buildings under such earthquakes. In previous studies regarding steel columns subjected to small amplitude cyclic loads, the deformation capacity of structural components used for high-rise buildings such as built-up box section columns and concrete-filled steel tube columns were evaluated in Japan since resonance with long-duration and long-period ground motions is significant in high-rise buildings. However, there are few researches focusing on the small amplitude behavior of cold-formed square hollow section (SHS) steel columns which are commonly used for Japanese low- and middle-rise steel buildings.

In this study, cyclic loading tests of SHS columns under small plastic deformation amplitude were conducted and the effect of the loading amplitude to deterioration behavior due to local buckling was investigated. Cold-formed SHS columns (BCR295 steel grade, nominal yield strength is 295 N/mm^2 and nominal tensile strength is 400 N/mm^2) were tested. The specimens were subjected to lateral force and constant compressive axial force. Test parameters were the loading history, the width-to-thickness ratio (D/t) and the compressive axial load ratio (N/N_y). D/t were set to 22.2 and 33.3; N/N_y were set to 0.2 and 0.35. Several constant small deformation amplitude cyclic loading histories, variable small deformation amplitude loading history and the monotonic loading history were employed.

The summary of this test results are as follows. The maximum strength of each specimen were determined by occurrence of local buckling and the strength deteriorated as the axial shortening of the plate in the local buckling zone progressed. The loading amplitude affected to the maximum strength and the strength deterioration behavior. The maximum strength decreased as the deformation amplitude became small. Meanwhile, the strength deterioration under small amplitude loading histories was smaller than that under the large amplitude loading history. The reason was that the progress of the axial shortening of the flange plate due to local buckling of each cycle is reduced because the effect of a tensile force induced due to bending become significant as the loading amplitude decrease. This phenomenon was more notable for specimens with a smaller D/t and N/N_y.

Keywords: Square Hollow Section Steel Column; Small Deformation Amplitude; Cyclic Loading Test; Local Buckling

1. Introduction

Structural components may be subjected to a relatively small amplitude and a large number of cyclic loading under long-duration and long-period earthquake excitations as well as multiple strong ground motions in a short period of time such as the 2016 Kumamoto Earthquake. Lower ends of columns of 1st story would yield under severe earthquake, even though the strong-column-weak-beam concept is adopted in the design. Therefore, deformation capacities and the hysteretic behaviors including the strength deterioration range of steel columns subjected to small amplitude cyclic loads should be clarified to evaluate seismic performance of buildings under such earthquakes.

In previous studies regarding steel columns subjected to small amplitude cyclic loads, the deformation capacity of structural components used for high-rise buildings such as built-up box section columns and concrete-filled steel tube columns were evaluated in Japan [1 - 3] since resonance with long-duration and long-period ground motions is significant in high-rise buildings. Meanwhile, there are few researches focusing on the small amplitude behavior of cold-formed square hollow section (SHS) steel columns which are commonly used for Japanese low- and middle-rise steel buildings [4].

In this study, cyclic loading tests of SHS columns under small plastic deformation amplitude are conducted and the effect of the loading amplitude to deterioration behavior due to local buckling is investigated.

2. Test Plan

2.1 Specimen and test setup

Test specimens were cold-roll-formed SHS columns (BCR295 steel grade, nominal yield strength is 295 N/mm^2 and nominal tensile strength is 400 N/mm^2) and the dimension of each specimen was □-200×200×9 or □-200×200×6. Results of the tensile coupon test of the flat part of SHS column using JIS-1A testing sample are shown in Fig. 1 and summarized in Table 1.

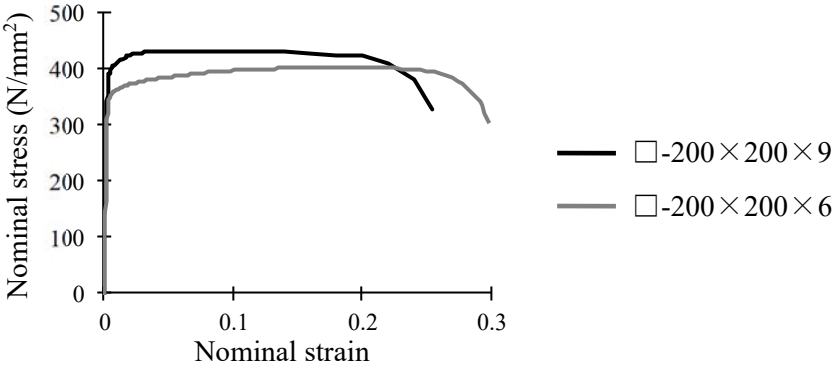

Fig. 1 – Stress-strain relationships

Table 1 – Tensile test results

Dimension	Yield stress (N/mm^2)	Tensile stress (N/mm^2)	Elongation (%)
□-200×200×9	392	430	26
□-200×200×6	345	403	30

The test setup is shown in Fig. 2. The upper end of the specimen was connected to the pin jig and the lower end was fixed to the loading table. The specimen was subjected to a lateral force by the horizontal jack. Constant compressive axial force was applied by three vertical jacks through the upper reaction frame and the vertical jacks were controlled so that the reaction frame keep horizontal. The horizontal jack was controlled by the column end rotation angle θ of the specimen.

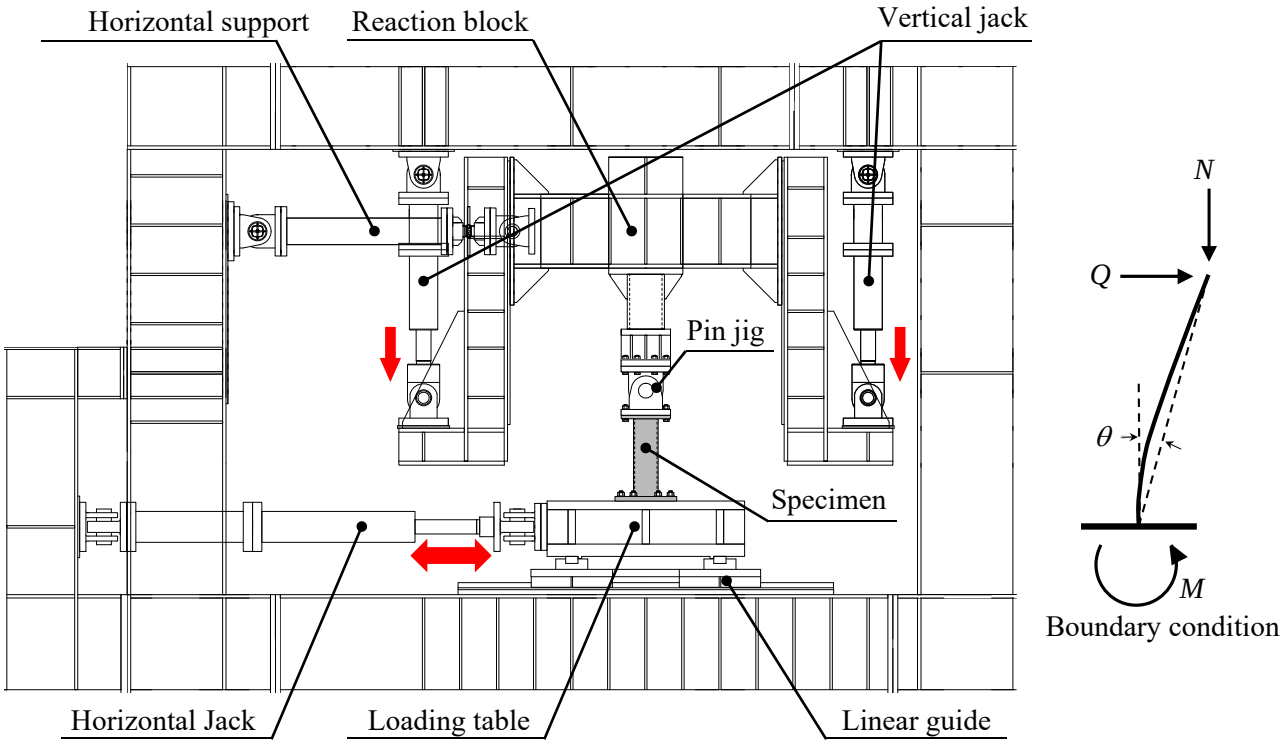

Fig. 2 – Test setup

2.2 Measurement

The load acting on the specimen was measured by the load cell installed in each jack, and the horizontal and the vertical deformation of the specimen were measured by displacement transducers. In addition, to measure the deformation of the local buckling zone as shown in Fig. 3, displacement transducers were installed at a position 1.1D (D is column depth) from the lower end of the specimen. The rotation angle, θ_b, and the axial deformation of the flange plate, δ_b, of the local buckling zone are calculated by Eq. (1), (2), respectively.

$$\theta_b = (d_2 - d_1) / L_b \tag{1}$$

$$\delta_b = \frac{d_1 + d_2}{2} + \frac{D}{2}\theta_b \tag{2}$$

where, d_1 and d_2 are vertical deformations at 1.1D from the lower end of the specimen, L_b is the horizontal distance between the displacement transducers which measure d_1 and d_2.

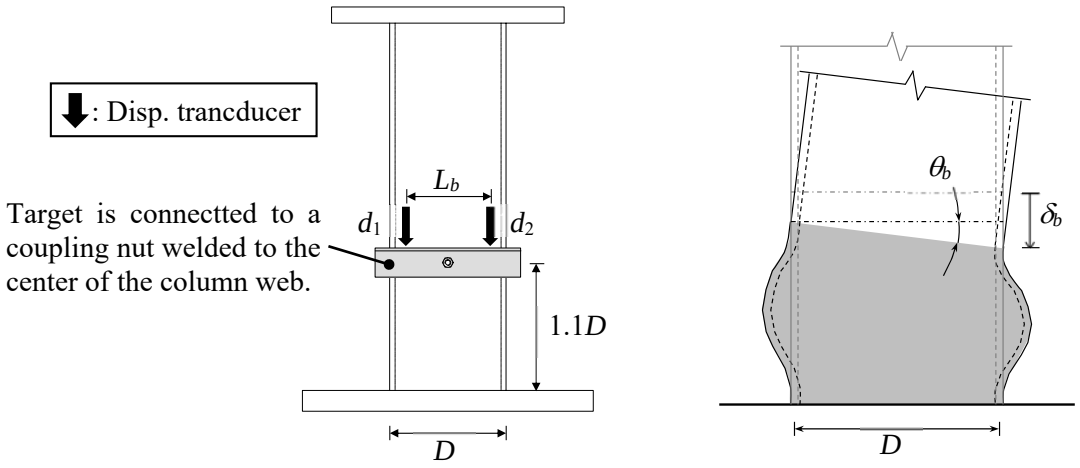

Fig. 3 – Measurement of the deformation of the local buckling zone

2.3 Test parameter

Test parameters are the width-to-thickness ratio (D/t) and the loading history. Test parameters are summarized in Table 2. Width-to-thickness ratios are 22.2 and 33.3. For D/t = 22.2 specimen, the axial load ratio, N/N_y, was set to 0.35. For D/t = 33.3 specimen, N/N_y was set to 0.2. Loading histories used in this test could be divided into three gropes: constant, variable, and monotonic deformation amplitude loading. For constant deformation amplitude, two peak-to-peak amplitudes were used: $1.5\theta_{pc}$, and $2.0\theta_{pc}$, where θ_{pc} is the calculated elastic rotation angle which corresponds the plastic moment considering the effect of the axial load. For variable deformation amplitude, one set was determined, and this set would be repeated. The peak-to-peak deformation amplitude of variable loading consisted of four cycles of $1.5\theta_{pc}$, two cycles of $2.0\theta_{pc}$, and one cycle of $2.5\theta_{pc}$, as shown in Fig. 4.

Table 2 – Test parameter

Specimen	Loading history	D/t	N/N_y
M_22.2_0.35	Monotonic	22.2	0.35
C1.5_22.2_0.35	1.5 θ_{pc} const.		
C2.0_22.2_0.35	2.0 θ_{pc} const.		
V_22.2_0.35	Variable amp. (see Fig. 4)		
M_33.3_0.2	Monotonic	33.3	0.2
C1.5_33.3_0.2	1.5 θ_{pc} const.		
C2.0_33.3_0.2	2.0 θ_{pc} const.		
V_33.3_0.2	Variable amp. (see Fig. 4)		

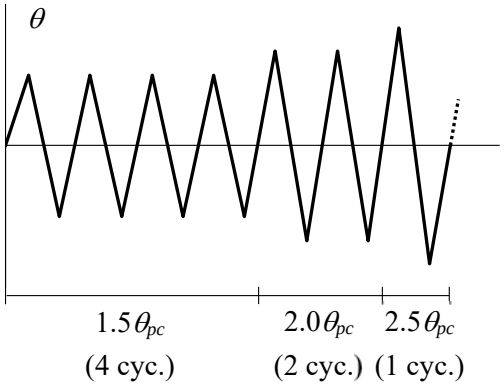

Fig. 4 – Variable amplitude loading history

3. Test Result

3.1 Load – deformation relationship and cumulative hysteresis curve

Fig. 5 shows column end moment, M, – rotation angle, θ, relationships and cumulative hysteresis curves for cyclic loading test results. $M - \theta$ relationships under monotonic loading is also shown by solid gray line in the graph which shows the cumulative hysteresis curve. Note that the cumulative hysteresis curve is obtained by connecting the skeleton curve before reaching the maximum strength and the hysteresis curve after reaching the maximum strength of each half cycle; the envelope curve of this cumulative hysteresis curve, which is defined as the extended skeleton curve, is empirically known that approximately corresponds to the hysteresis curve under monotonic loading [5].

The strength of each specimen deteriorated as progress local buckling. The strength deterioration behavior after reaching the maximum strength of C2.0_33.3_0.2 and V_33.3_0.2 specimen roughly corresponds to that of the monotonic loading. However, with respect to the other specimens subjected to cyclic load, the number of cycles from after reaching the maximum strength until initiating the obvious deterioration of the strength increased. Moreover, the negative slope of the envelope curve of those specimens after observed the strength deterioration obviously was gentler than that of the specimen subjected to monotonic load. As a result, the deterioration behavior of those specimen did not correspond to the behavior of the monotonic loading test result.

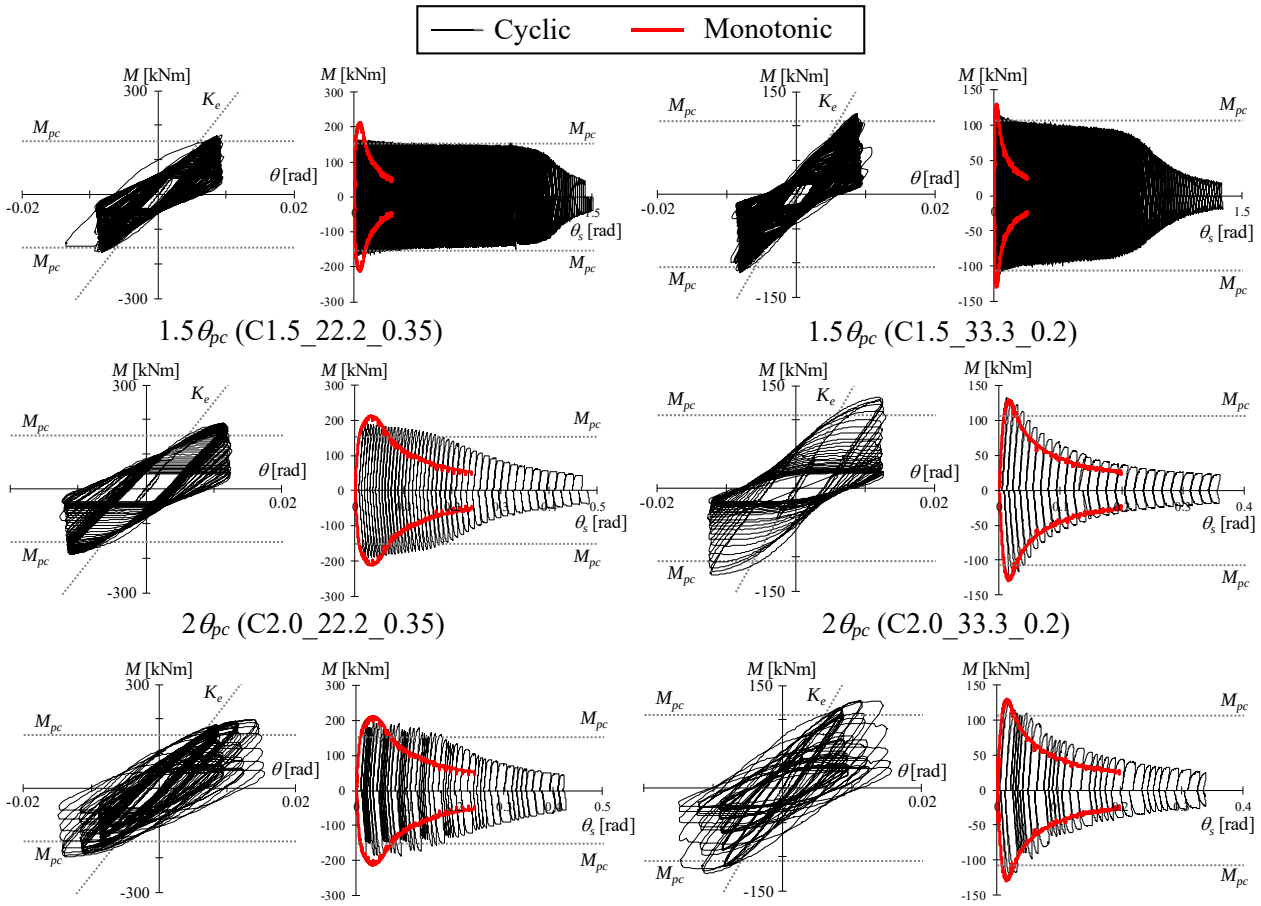

(a) $D/t = 22.2$, $N/N_y = 0.35$ (b) $D/t = 33.3$, $N/N_y = 0.2$

Fig. 5 – Load – deformation relationship and cumulative hysteresis curve

3.2 Axial deformation of the flange plate in the local buckling zone

Column end moment, M, and the axial deformation of the flange plate in the local buckling zone, δ_b, relationships are shown in Fig. 6. The increment of δ_b of each half cycle under cyclic loading became large as the strength got deteriorate. The envelope curve of $M - \delta_b$ relationship under positive bending moment for each cyclic loading test result approximately corresponds to $M - \delta_b$ relationship under monotonic loading, that is, the strength deterioration due to local buckling is dependent on δ_b regardless of loading history.

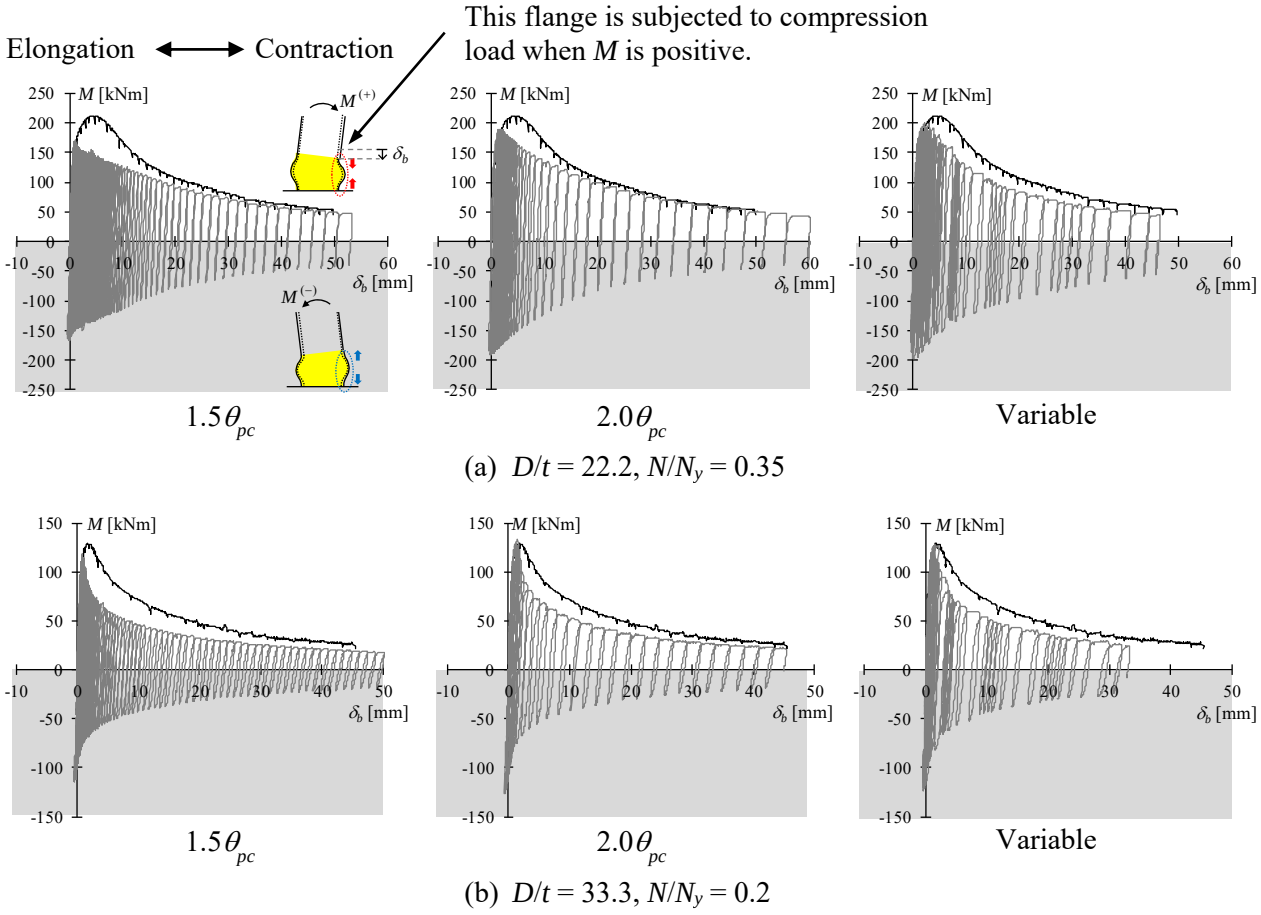

Fig. 6 – Axial deformation of the flange plate in the local buckling zone

To investigate the progress of δ_b for each half cycle, the ratio of the rotation angle due to axial shortening of the flange plate in the local buckling zone of each half cycle, $\Delta\theta_{bc}$, to the rotation angle of the local buckling zone of each half cycle, $\Delta\theta_b$, was calculated (see Fig. 7). $\Delta\theta_{bc}$ is obtained by Eq. (3).

$$\Delta\theta_{bc} = \Delta\delta_{bc} / D \tag{3}$$

where, Δ denotes the increment of half cycle and $\Delta\delta_{bc}$ is the increment of the axial shortening of the flange plate in the local buckling zone of half cycle. Note that $\Delta\theta_{bc}/\Delta\theta_b = 0.5$ indicates the axial elongation and shortening of the flange plate in the local buckling zone of a half cycle, which are caused by tensile and compression load due to bending, respectively, are equal; $\Delta\theta_{bc}/\Delta\theta_b > 0.5$ indicates that the axial shortening in the local buckling zone increases.

Fig. 8 shows $\Delta\theta_{bc} / \Delta\theta_b - \delta_b$ relationships for the cyclic loading test results. Also, δ_b of the monotonic loading test result when reaching the maximum strength (hereafter, $\delta_{b,u}$) and $\Delta\theta_{bc}/\Delta\theta_b = 0.5$ are also shown by black broken line and gray broken line in Fig. 8, respectively. $\Delta\theta_{bc}/\Delta\theta_b$ was approximately constant and ranged from 0.5 to 0.6 until δ_b reaches $\delta_{b,u}$ of the monotonic loading test result. However, after δ_b reaches $\delta_{b,u}$, $\Delta\theta_{bc}/\Delta\theta_b$ was significantly increase; that is; the cyclic behavior is no longer stable due to the progress of local buckling. Hereafter, the point when δ_b reaches $\delta_{b,u}$, is defined as ”stable limit”.

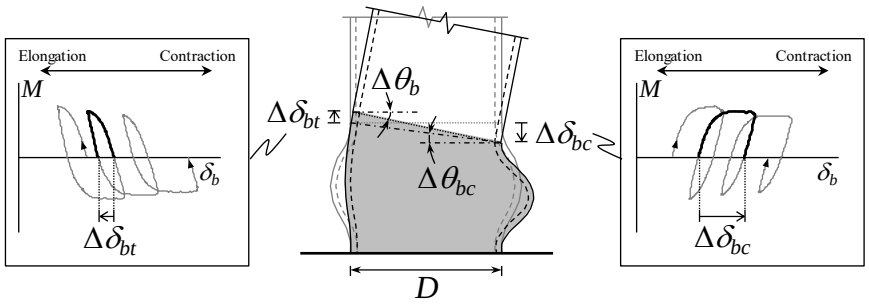

Fig. 7 – Definition of $\Delta\theta_b$ and $\Delta\theta_{bc}$

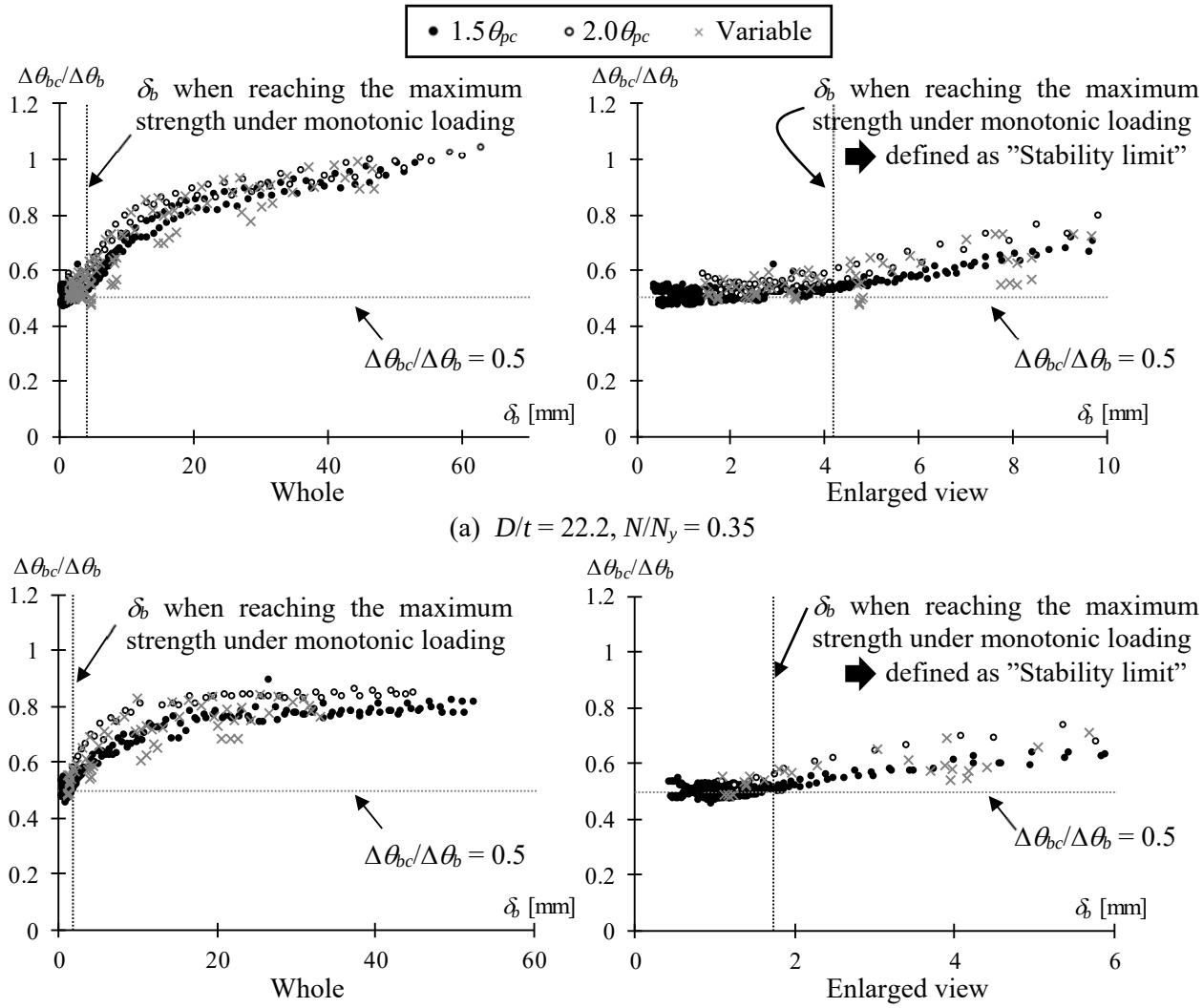

(a) $D/t = 22.2$, $N/N_y = 0.35$

(b) $D/t = 33.3$, $N/N_y = 0.2$

Fig. 8 – $\Delta\theta_{bc}/\Delta\theta_b - \delta_b$ relationship

4. Modification of the extended skeleton curve

The modification method of the extended skeleton curve under small deformation amplitude loading is proposed based on the stable limit and the ratio $\Delta\theta_{bc}/\Delta\theta_b$. Fig. 9 shows the schematic diagram of the modification method of the extended skeleton curve. First, since the progress of the axial shortening of the flange part in the local buckling zone is small and the strength deterioration can be assumed to be negligible before reaching the stable limit, the cumulative deformation which is from after reaching the maximum strength to reaching the stability limit is eliminated from the extended skeleton curve. Also, the extended skeleton curve after reaching the stable limit is offset by $\theta_{s,cr} - \theta_u$ from the original position as shown in Fig. 9 (a). In which $\theta_{s,cr}$ is the deformation of the extended skeleton curve when reaching the stability limit under cyclic loading and θ_u is the deformation corresponding to the maximum strength under monotonic loading.

Fig. 6 showed that the strength deterioration after reaching the stability limit is governed by the axial shortening of the flange plate in the local buckling zone regardless of loading histories; however, the deformation of the extended skeleton curve after reaching the stability limit includes both axial shortening and elongation components due to bending. Therefore, since only the axial shortening component can be assumed to affect to the deterioration behavior due to local buckling, a half cycle increment of the deformation of the extended skeleton curve is modified by multiplying the ratio $\Delta\theta_{bc}/\Delta\theta_b$ of each half cycle, as shown in Fig. 9 (b).

Fig. 10 shows comparisons of the modified extended skeleton curve and hysteresis curve under monotonic loading. The deterioration behavior corresponds regardless of loading history.

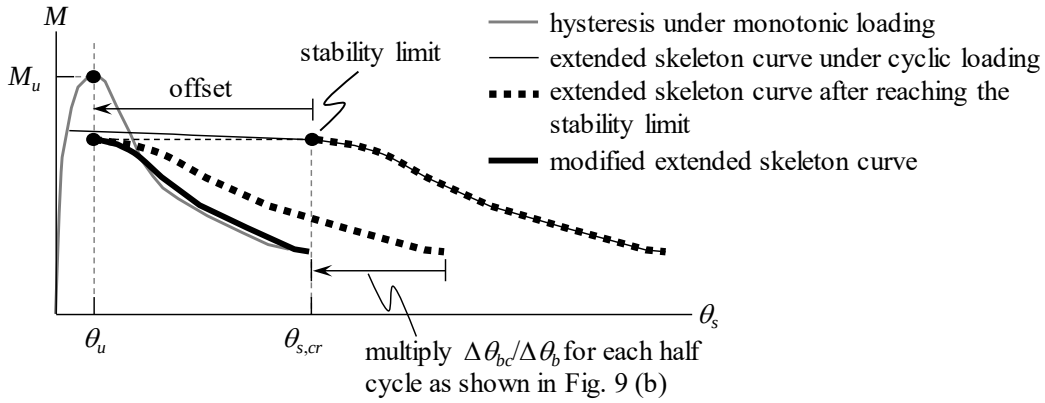

(a) Schematic diagram of modification

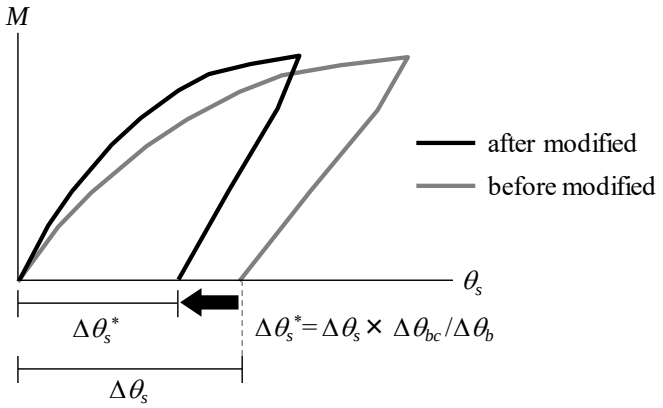

(b) Modification of each half cycle's $\Delta\theta_s$ after reaching the stability limit

Fig. 9 – Modification method of the extended skeleton curve

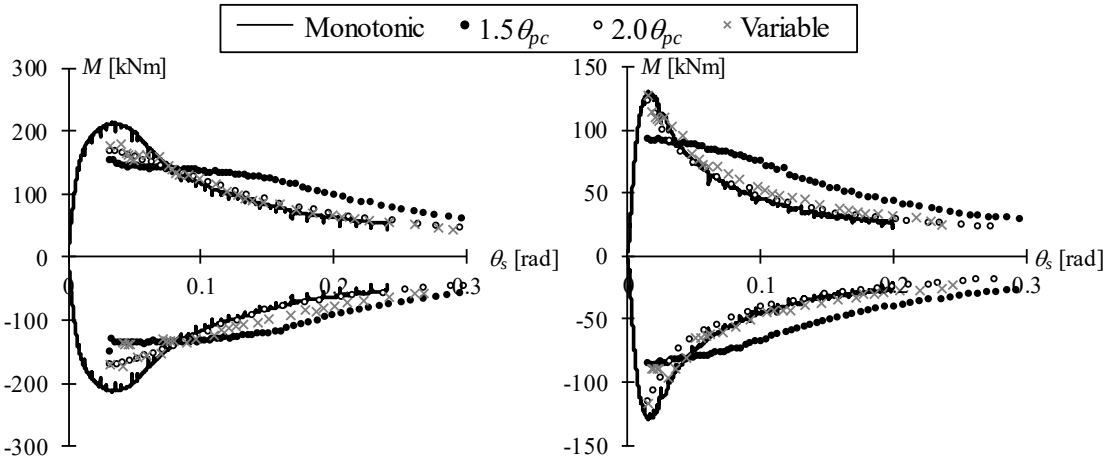

Figure 10 – Comparison of the modified extended skeleton curve and the hysteresis curve under monotonic loading

5. Conclusions

In this study, cyclic loading tests under small deformation amplitude were conducted and the strength deterioration behavior was investigated.

1) The strength of each specimen deteriorated due to local buckling. Comparing extended skeleton curves under cyclic loading and hysteresis curve under monotonic loading, the strength deterioration was reduced as the decrease of the deformation amplitude. Especially, the strength deterioration behavior of the amplitude of $1.5\theta_{pc}$ significantly differ because the number of cycles from after reaching the maximum strength until initiating the obvious deterioration of the strength significantly increased.
2) The strength deterioration was dependent on the axial shortening of the flange plate in the local buckling zone, δ_b, regardless of loading history.
3) After δ_b under cyclic loading exceeded $\delta_{b,u}$ of the monotonic loading test result, the ratio of the rotation angle due to axial shortening of the flange plate in the local buckling zone of each half cycle, $\Delta\theta_{bc}$, to the rotation angle of the local buckling zone of each half cycle, $\Delta\theta_b$, was significantly increase. Therefore, the point when δ_b under cyclic loading reaches $\delta_{b,u}$, can be defined as "stable limit".
4) The extended skeleton curve was modified based on the stable limit and the ratio $\Delta\theta_{bc}/\Delta\theta_b$, as follows. (A) The extended skeleton curve after reaching the stability limit is offset. The offset distance is set to $\theta_{s,cr} - \theta_u$ in which $\theta_{s,cr}$ is the deformation of the extended skeleton curve when reaching the stability limit under cyclic loading and θ_u is the deformation corresponding to the maximum strength under monotonic loading. (B) A half cycle increment of the deformation of the extended skeleton curve after reaching the stability limit is modified by multiplying the ratio $\Delta\theta_{bc}/\Delta\theta_b$ of each half cycle.
5) The modified extended skeleton curve corresponded to the hysteresis curve under monotonic loading regardless of loading history.

6. Acknowledgement

This experiment is financially supported by the Japan Iron and Steel Federation and JSPS KAKENHI Grant Number 17H01302.

7. References

[1] Kiyokawa T. et al. (2011) (2012): Study on safety assessment methods for super-high-rise steel buildings against long-period earthquake ground motions Part 6 – 7, Part 13 – 14. *Summaries of Technical Paper of Annual Meeting*, Architectural Institute of Japan, 1023-1026, 1057-1060. (in Japanese)

[2] Narihara H. et al. (2014): Study on safety assessment methods for super-high-rise steel buildings against long-period earthquake ground motions Part 27 – 31. *Summaries of Technical Paper of Annual Meeting*, Architectural Institute of Japan, 1251 – 1260. (in Japanese)

[3] Kido M., Tsuda K., Fukumoto T., Ichinohe Y., Morita K. (2019): Behavior of square concreate filled steel tubular beam-columns subjected to lateral load with constant cyclic displacement, *Journal of Structural and Construction Engineering*, Volume 84 (Number 759), 725-735. (in Japanese)

[4] Kuwamura H., Iyama J., Zhu D. (1999): Collapse and residual drift during post-local-buckling behaviors under earthquake. *Journal of Structural and Construction Engineering*, Volume 64 (Number 526), 169-176. (in Japanese)

[5] Yamada S., Ishida T., Jiao Y (2018): Hysteretic behavior of RHS columns under random cyclic loading considering local buckling. *International Journal of Steel Structures*, Volume 18 (Number 5), 1761-1771.

